Journal of Cardiovascular Magnetic Resonance 27 (2025) 101135

Contents lists available at ScienceDirect

Journal of Cardiovascular Magnetic Resonance

journal homepage: www.sciencedirect.com/journal/jocmr

Original Research

Comprehensive prognosis assessment of cardiovascular magnetic resonance parametric mapping in light chain amyloidosis

Xiao Li[a,1], Yubo Guo[a,1], Kaini Shen[b,1], Sisi Huang[c], Yajuan Gao[b], Lu Lin[a], Jian Wang[a], Jian Cao[a], Xinxin Cao[b], Zhengyu Jin[a], Zhuoli Zhang[d], Akos Varga-Szemes[e], U. Joseph Schoepf[e], Jian Li[b,*], Yining Wang[a,**]

[a] Department of Radiology, State Key Laboratory of Complex Severe and Rare Diseases, Peking Union Medical College Hospital, Chinese Academy of Medical Sciences & Peking Union Medical College, Beijing, China
[b] Department of Hematology, State Key Laboratory of Complex Severe and Rare Diseases, Peking Union Medical College Hospital, Chinese Academy of Medical Sciences & Peking Union Medical College, Beijing, China
[c] Department of Radiology, Sun Yat-sen University Cancer Center, Guangzhou, China
[d] Department of Radiological Sciences, University of California, Irvine, California, USA
[e] Division of Cardiovascular Imaging, Department of Radiology and Radiological Science, Medical University of South Carolina, Charleston, South Carolina, USA

ARTICLE INFO

Keywords:
Amyloidosis
Cardiovascular magnetic resonance
Survival analysis

ABSTRACT

Background: Recent evidence underscores the importance of cardiovascular magnetic resonance (CMR) in light chain amyloidosis (AL amyloidosis). We aimed to comprehensively assess the prognostic significance of CMR parametric mapping in AL amyloidosis.

Methods: This prospective study consecutively included AL amyloidosis patients who underwent CMR imaging before therapy. The statistical analyses included T2, extracellular volume, and native T1 as variates under investigation, adjusted for well-established prognostic markers. The outcome was death from any cause.

Results: In total, 195 patients (age, 57.2 ± 9.1 years; male/female, 123/72) were recruited. At the median follow-up time (19 months), the survival probability was approximately 67.2% (131/195). T > 44 ms, extracellular volume fraction (ECV) > 47%, and native T1 > 1468 ms were significantly prognostic (all, $P < 0.05$) but non-significant after adjustment for N-terminal pro-B-type natriuretic peptide (all, $P > 0.05$) in AL amyloidosis. T2 > 44 ms was independently prognostic after correcting for left ventricle (LV) late gadolinium enhancement, LV ejection fraction, LV longitudinal strain, and therapeutic response (all, $P < 0.05$). In patients achieving deep hematologic response, T2 > 44 ms (hazard ratios [HR] 6.611, 95% confidence interval [CI] 1.723–25.361, $P = 0.006$) was significantly prognostic for mortality after adjustment for cardiac response. Accordingly, T2 > 44 ms was significantly associated with mortality (HR 5.734, 95% CI 1.189–27.656, $P = 0.030$) and remained independently prognostic after correcting for LV late gadolinium enhancement and LV longitudinal strain (both, $P < 0.05$) in patients who achieved both deep hematologic response and cardiac response.

Conclusion: This study highlights that T2 is a valuable independent predictor of mortality in an AL amyloidosis population, additive to common CMR risk factors. Moreover, myocardial edema assessment identified patients in need of adjunctive therapies, which is of particular prognostic significance in patients with deep therapeutic response.

Abbreviations: AL amyloidosis, light chain amyloidosis; bSSFP, balanced steady-state free precession; CI, confidence interval; CMR, cardiovascular magnetic resonance; CR, complete response; cTn, cardiac troponin; dFLC, difference between involved and uninvolved FLC; ECV, extracellular volume fraction; EF, ejection fraction; FA, flip angle; FLC, free light chain; HR, hazard ratios; LGE, late gadolinium enhancement; LV, left ventricle; LVEF, left ventricular ejection fraction; MOLLI, modified Look-Locker inversion-recovery; NYHA, New York Heart Association; NT-proBNP, N-terminal pro-B-type natriuretic peptide; OR, organ response; PD, progressive disease; PR, partial response; RV, right ventricle; RVEF, right ventricular ejection fraction; SD, stable disease; TE, echo time; TR, repetition time; VGPR, very good partial response

* Corresponding author. Department of Hematology, Peking Union Medical College Hospital, No.1, Shuaifuyuan, Dongcheng District, Beijing 100730, China.
** Corresponding author. Department of Radiology, Peking Union Medical College Hospital, No.1, Shuaifuyuan, Dongcheng District, Beijing 100730, China.
E-mail addresses: lijian@pumch.cn (J. Li), wangyining@pumch.cn (Y. Wang).
[1] Co-first authors.

https://doi.org/10.1016/j.jocmr.2024.101135
Received 10 November 2023; Received in revised form 7 December 2024; Accepted 10 December 2024

1. Background

Light chain amyloidosis (AL amyloidosis) is characterized by the deposition of misfolded light chains in various tissues and organs, which causes structural damage and progressive dysfunction [1]. Cardiac involvement is common and one of the main determinants of survival [2]; thus, risk stratification and follow-up focusing on the heart are of vital importance. Currently, consensus guidelines assess prognosis and responses to treatment based on serum or urine free light chain (FLC) ratio, cardiac troponin (cTn) level, N-terminal pro-B-type natriuretic peptide (NT-proBNP) level, New York Heart Association (NYHA) class and ejection fraction (EF) [3–5], but none of them reflect the myocardial amyloid burden directly.

Cardiovascular magnetic resonance (CMR) imaging offers one-stop multiparametric analysis of cardiac structure and function, as well as myocardial tissue characterization based on late gadolinium enhancement (LGE) and parametric mapping [6]. The prognostic value of CMR-derived parameters has been established [7–12], yet there is no consensus as to whether CMR parametric mapping offers prognostic advantage in AL amyloidosis. The aim of this study was to comprehensively assess the prognostic significance of CMR parametric mapping in an AL amyloidosis population.

2. Methods

2.1. Study population

This prospective study consecutively included AL amyloidosis patients who underwent CMR imaging before therapy at our hospital between August 1, 2014 and December 31, 2019. Patients were excluded if they had no cardiac involvement or a magnetic resonance study was contraindicated (claustrophobia, metallic implants, glomerular filtration rate < 45 mL/[min·1.73 m^2]). All patients had biopsy–proven AL amyloidosis based on positive Congo red staining, immunohistochemical staining, immunofluorescence, or mass spectrometry. The assays were performed in the tissues listed as follows: kidney (n = 112), myocardium (n = 59), tongue (n = 21), liver (n = 20), fat (n = 13), buccal mucosa (n = 10), bone marrow (n = 9), upper gastrointestinal tract (n = 7), lymph nodes (n = 3), skin (n = 3), muscle (n = 2), rectum (n = 2), peripheral nerve (n = 1) and lung (n = 1). All patients underwent assessment of cardiac troponin I (cTnI), N-terminal pro-brain natriuretic peptide (NT-proBNP), and serum FLC differences at baseline and were categorized based on the revised Mayo Stage published in 2012 [5]. Cardiac involvement was established as 1) endomyocardial biopsy–proven cardiac amyloidosis; and 2) extracardiac biopsy–proven amyloidosis, NT-proBNP > 332 pg/mL or left ventricle (LV) mean wall thickness > 12 mm in the absence of hypertension or other potential causes of LV hypertrophy [13,14].

The institutional ethics committee at Peking Union Medical College Hospital (Beijing, China) approved the study. All participants were required to provide written informed consent before recruitment.

2.2. CMR scanning protocol

CMR imaging was performed using a 3T whole-body magnetic resonance imaging system (Magnetom Skyra, Siemens Healthineers, Erlangen, Germany). The cine images were acquired using an electrocardiogram-gated two-dimensional (2D) balanced steady-state free precession (bSSFP) sequence during multiple breath holds. Two-, three-, and four-chamber long-axis views and short-axis views including 9–11 slices were acquired. The key parameters were as follows: repetition time (TR)/echo time (TE), 3.3 ms/1.43 ms; flip angle (FA), 55°–70°; voxel size, 1.6 × 1.6 × 8.0 mm^3, gap of 2 mm; temporal resolution, 45.6 ms; and bandwidth, 962 Hz/pixel. Native and 15 min postcontrast T1 mapping were acquired using a modified Look-Locker inversion-recovery (MOLLI) sequence with a four-chamber long-axis slice and basal, mid, and apical short-axis slices matching the cine images. Acquisition scheme 5(3)3 and 4(1)3(1)2 were used for native and postcontrast T1 mapping, respectively. The other parameters included repetition time/echo time/flip angle (TR/TE/FA), 2.7 ms/1.12 ms/20°; and voxel size, 1.4 × 1.4 × 8.0 mm^3. T2 mapping was acquired using a T2-prepared single-shot bSSFP sequence with slice positions matching the T1 mapping images. Three single-shot bSSFP images with different T2 preparation times (TE_{T2P} = 0 ms, 25 ms, 55 ms) were obtained at the end-diastolic phase during a single breath hold. The key parameters were as follows: TR/TE/FA, 2.4 ms/1.0 ms/70°; field of view, 320–340 × 262–278 mm^2; slice thickness, 8 mm; and bandwidth, 1093 Hz/px. Ten-minute postcontrast LGE images were acquired using a 2D phase-sensitive inversion-recovery gradient-echo pulse sequence, with the slice position matching the cine images [6,15]. LGE images were acquired using phase-sensitive inversion-recovery gradient-echo pulse sequence in long-axis and short-axis views 10 min after intravenous administration of gadopentetate dimeglumine (Beijing Beilu Pharmaceutical; dose, 0.15 mmol/kg).

2.3. CMR image analysis

Standard parameters of cardiac structure and function, myocardial deformation, native T1 and T2, and extracellular volume fraction (ECV) were measured semiautomatically using dedicated CMR software (cvi42 version 5.3; Circle Cardiovascular Imaging, Calgary, Alberta, Canada). The parameters of cardiac structure and function were measured by segmenting the endocardial and epicardial borders in long-axis and short-axis cine at the end-systole and end-diastole [16]. Global and segmental strain parameters were automatically calculated by the software, including the radial strain and circumferential strain from short-axis cine slices, and longitudinal strain from three long-axis cine slices. The endocardial and epicardial borders in the end-diastole phase were chosen, and the borders for subsequent phase imaging were automatically created. Global left ventricular (LV) T1 and T2 values were measured as average of three short-axis stacks by contouring the endocardium and epicardium on inline-generated parametric maps. An offset of 5% was used from set contours to avoid signal contamination. The local normal ranges were 1295.0 ± 36.2 ms for native T1 and 40.3 ± 2.3 ms for T2 [17]. ECV values were obtained from pre- and post-contrast T1 maps indexing for hematocrit, measured within 3 days before each CMR study. The LV LGE pattern was classified into negative, subendocardial, and transmural groups [18]. The right ventricular (RV) LGE pattern was classified into negative and positive groups. Two experienced radiologists independently assessed LGE CMR images, and discrepancies were resolved in consensus during a joint evaluation with a third radiologist.

2.4. Clinical follow-up

A hematologist blinded to the CMR results conducted the telephone and clinical follow-up every 3 months. All patients received bortezomib or melphalan-based first-line chemotherapy. All patients underwent assessment of the cTnI level, NT-proBNP level, and serum and urine FLC ratios upon follow-up, and were categorized based on criteria for response to treatment published in 2012 [3]. Hematologic responses were graded as follows: 1) complete response (CR) to normal FLC levels, normal kappa/lambda ratio, and negative serum and urine immunofixation; 2) very good partial response (VGPR), difference between involved and uninvolved FLC (dFLC) reduced to < 40 mg/L; and 3) partial response, dFLC reduced by > 50%. Cardiac responses were defined as NT-proBNP decrease > 30% and > 300 ng/L if baseline NT-proBNP ≥650 ng/L or NYHA class decrease ≥ two-class if baseline NYHA class 3 or 4. Optimal hematologic and cardiac responses to therapy were used for statistical analysis. The outcome was death from any cause. The last clinic visit record was used if patients were lost to follow-up.

2.5. Statistical analysis

Statistical analysis was performed using IBM SPSS Statistics (version 21.0, IBM Corp, Armonk, New York). All continuous variables are

presented as mean ± SD, except for cTnI, NT-proBNP, and FLC differences, which are presented as medians (quartiles 1–quartiles 3). Survival was evaluated with Cox proportional hazards regression analysis and Kaplan-Meier curve, the cutoffs were defined as mean values of T2, T1, and ECV in the present cohort. Univariable Cox proportional hazard models were used to assess the association between variates and outcome, providing estimated hazard ratios (HR) with 95% confidence interval (CI). Statistically significant predictors of outcome were entered into a multivariable Cox proportional hazards analysis with forward stepwise selection to determine which variates were independent predictors of mortality. As this study focuses on the prognostic value of parametric mapping, the statistical analyses included T2, ECV, and native T1 as variates under investigation, adjusted for well-established prognostic markers. In analyses where the comparator had zero events and the partial likelihood converged to a finite value, we applied Firth's penalized partial likelihood correction to Cox regression models. The mean value was used as cutoff values. A two-tailed *P* value of less than 0.05 was considered statistically significant.

3. Results

3.1. Characteristics and survival analysis in all AL amyloidosis patients

In total, 195 patients (age, 57.2 ± 9.1 years; male/female, 123/72) were recruited. Representative case examples of patients with different degrees of disease severity are shown in Fig. 1. At the time of last follow-up, 125 (64.1%) patients were alive, with a survival probability of approximately 67.2% (131/195) at the median follow-up time (19 months). Three patients were lost to follow-up. Table 1 and Supplemental Table 1 show the characteristics and Cox analysis in all patients.

Univariate Cox proportional hazard analysis showed that biventricular EF and strain, LGE and parametric mapping were significantly associated with mortality. In the multivariable-adjusted competing risk model, only NT-proBNP (HR: 1.948 [95% CI: 1.456–2.607; $P < 0.001$]) and cTnI (HR: 1.345 [95% CI: 1.128–1.603; $P = 0.001$]) remained independent predictors. Furthermore, parametric mapping's predictive value was evaluated when known clinical predictors were added. Table 2 summarizes the multivariate Cox proportional hazard analysis including T2, ECV, and native T1, adjusted for well-established prognostic markers. T2 > 44 ms, ECV > 47%, and native T1 > 1468 ms were no longer statistically significant after adjustment for NT-proBNP (all, $P > 0.05$). T2 > 44 ms and ECV > 47% remained independently prognostic after adjustment for cTnI (both, $P < 0.05$). T2 > 44 ms was independently prognostic after correcting for LV LGE, LVEF, LV longitudinal strain, and therapeutic response (all, $P < 0.05$).

Kaplan-Meier curve analysis demonstrated that patients with T2 > 44 ms had significantly lower rates for overall survival (log rank, $P = 0.019$; Fig. 2A) than those with T2 ≤44 ms. Also, patients with ECV ≤47% and ECV > 47% differed significantly in survival probability (log rank, $P = 0.006$; Fig. 2B); patients with T1 ≤1468 ms and T1 > 1468 ms differed significantly in survival probability (log rank, $P = 0.038$; Fig. 2C).

3.2. Survival analysis in patients with different Mayo stages

There were 28 (14.4%), 44 (22.6%), 69 (35.4%), and 54 (27.6%) patients categorized as Mayo stages I, II, III, and IV, respectively. At the time of last follow-up, 26 (92.9%) patients with Mayo I, 30 (68.2%) patients with Mayo II, 43 (62.3%) patients with Mayo III, and 26 (48.1%) patients with Mayo IV were alive. Table 3 summarizes the univariable and multivariate Cox proportional hazards analysis of overall survival in the Mayo stage subgroups. Multivariate-adjusted analysis showed that in Mayo stage II patients, ECV > 47% was a significant prognostic factor for mortality after correcting for therapeutic response and LVEF (both, $P < 0.05$); in Mayo stage IV patients, T2 > 44 ms (HR 4.177, 95% CI 1.122–15.545, $P = 0.033$) was a significant prognostic factor for mortality after correcting for therapeutic response.

3.3. Survival analysis in patients achieving hematologic and cardiac responses

There were 82 (42.1%), 40 (20.5%), 18 (9.2%), and 20 (10.3%) patients who achieved hematologic CR, VGPR, partial response, and stable disease, respectively. Thirty-five (17.9%) patients had no hematologic response data mainly because of an early death. Patients with CR and VGPR were grouped into a deep hematologic response subgroup. At the time of last follow-up, 108 of 122 (88.5%) patients in the subgroup were alive, 90 of which achieved cardiac response. Table 4 summarizes the univariable and multivariate Cox proportional hazards analysis of overall survival among the patients achieving hematologic and cardiac response. Multivariate analysis showed that in patients achieving deep hematologic response, T2 > 44 ms (HR 6.611, 95% CI 1.723–25.361, $P = 0.006$) was significantly prognostic for mortality after adjustment for cardiac response. Accordingly, univariate analysis

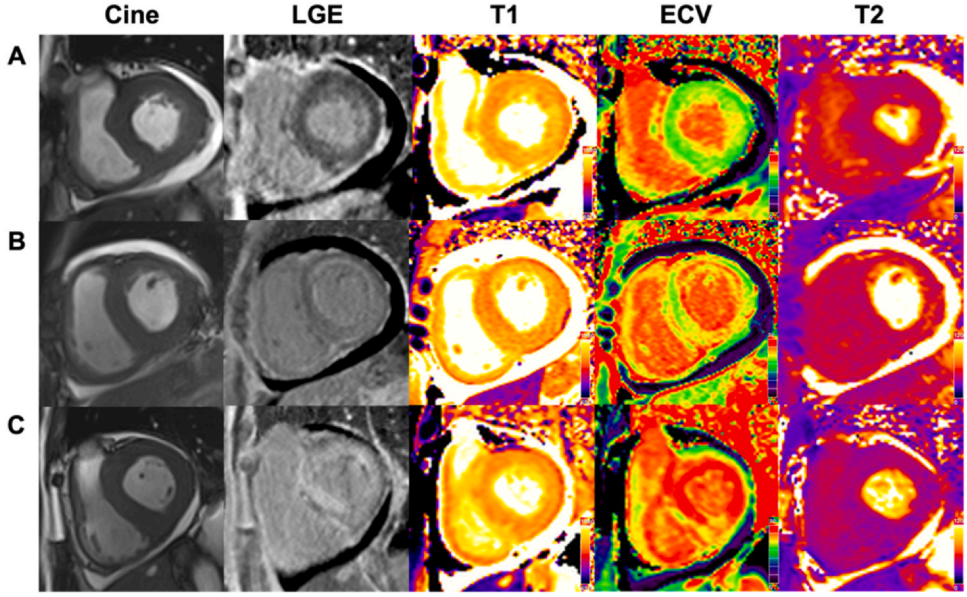

Fig. 1. Representative examples of patients with different disease severities. (A) A 60-year-old female with Mayo stage II, subendocardial LGE, native T1 of 1544 ms, T2 of 47 ms, and ECV of 43%, reached the endpoint at 1 month. (B) A 62-year-old female with Mayo stage III, subendocardial LGE, native T1 of 1501 ms, T2 of 51 ms, and ECV of 52%, reached the endpoint at 7 months. (C) A 78-year-old male with Mayo stage III, transmural LGE, native T1 of 1473 ms, T2 of 39 ms, and ECV of 56%, reached the endpoint at 4 months. *LGE* late gadolinium enhancement, *ECV* extracellular volume fraction

Table 1
Demographic, clinical, and CMR characteristics and Cox analysis in all 195 patients.

	All (N = 195)	Survivors (n = 125)	Endpoint (n = 70)	*P*	Univariable analysis		Stepwise multivariable analysis	
					HR (95% CI)	*P*	HR (95% CI)	*P*
Age, years	57.2 ± 9.1	57.1 ± 8.8	57.5 ± 9.7	0.430	1.006 (0.979, 1.033)	0.680		
Male/female	123/72	74/51	49/21	0.134	0.644 (0.386, 1.075)	0.092		
cTnI, μg/L	0.077 (0.030, 0.169)	0.059 (0.024, 0.127)	0.121 (0.042, 0.231)	0.001	1.309 (1.123, 1.526)	0.001	1.345 (1.128, 1.603)	0.001
NT-proBNP, pg/mL	2795 (1288, 4776)	2130 (828, 3722)	4446 (2498, 8418)	< 0.001	—	—		
Ln (NT-proBNP)	—	—	—	—	2.025 (1.569, 2.613)	< 0.001	1.948 (1.456, 2.607)	< 0.001
dFLC, mg/L	220 (106, 461)	216 (98, 471)	249 (113, 466)	0.506	—	—		
Ln (dFLC)	—	—	—	—	1.130 (0.916, 1.394)	0.253		
Mayo stage, I/II/III/IV	28/44/69/54	26/30/43/26	2/14/26/28	0.001	1.662 (1.280, 2.159)	< 0.001		
NYHA class, I/II/III/IV	49/80/56/10	36/55/29/5	13/25/27/5	0.067	1.425 (1.084, 1.873)	0.011		
LV end-diastolic volume index	76.1 ± 17.0	75.5 ± 17.4	77.0 ± 16.3	0.760	1.005 (0.991, 1.019)	0.472		
LV end-systolic volume index	35.0 ± 13.8	33.4 ± 13.0	37.9 ± 14.7	0.238	1.019 (1.004, 1.035)	0.016		
LA volume, mL	71.7 ± 30.6	69.3 ± 29.32	75.9 ± 32.5	0.242	1.005 (0.998, 1.012)	0.172		
LVEF, %	54.8 ± 11.5	56.3 ± 10.9	51.9 ± 12.1	0.215	0.972 (0.953, 0.991)	0.005		
LV radial strain, %	22.6 ± 10.9	24.7 ± 11.6	18.8 ± 8.4	0.009	0.955 (0.930, 0.980)	0.001		
LV circumferential strain, %	−16.8 ± 4.7	−17.7 ± 4.8	−15.3 ± 4.2	0.267	1.096 (1.042, 1.154)	< 0.001		
LV longitudinal strain, %	−8.5 ± 3.6	−9.2 ± 3.6	−7.3 ± 3.2	0.075	1.138 (1.054, 1.228)	0.001		
Index LV mass, g/m^2	71.4 ± 19.5	70.1 ± 30.4	73.8 ± 17.5	0.341	1.008 (0.996, 1.020)	0.185		
Septal thickness, mm	16.8 ± 4.2	19.2 ± 3.8	14 ± 4.4	0.429	1.005 (0.993, 1.017)	0.428		
T2, ms	43.5 ± 3.3	43.3 ± 3.1	44.1 ± 3.6	0.437	1.061 (0.980, 1.148)	0.145		
T2, > 44 ms	105 (54)	62 (50)	43 (61)	0.030	1.846 (1.085, 3.142)	0.024		
ECV, %	46.7 ± 8.4	45.4 ± 8.1	49.0 ± 8.5	0.496	1.045 (1.014, 1.076)	0.004		
ECV, > 47%	102 (52)	63 (50)	399 (56)	0.013	1.929 (1.183, 3.145)	0.008		
Native T1, ms	1467.8 ± 92.1	1464.3 ± 87.9	1473.9 ± 99.4	0.982	1.001 (0.998 , 1.004)	0.445		
Native T1, > 1468 ms	90 (46)	55 (44)	35 (50)	0.029	1.668 (1.014, 2.744)	0.044		
LV LGE, none/subendocardial/transmural	12/69/114	11/49/65	1/20/49	0.019	1.849 (1.179, 2.899)	0.007		
RV end-diastolic volume index	67.7 ± 18.1	68.2 ± 18.3	66.9 ± 17.9	0.531	0.997 (0.983, 1.010)	0.646		
RV end-systolic volume index	33.7 ± 15.5	32.5 ± 15.3	66.9 ± 17.9	0.680	1.011 (0.997, 1.026)	0.122		
RA volume, mL	77.8 ± 32.4	32.5 ± 15.3	35.9 ± 15.6	0.811	1.009 (1.002, 1.015)	0.009		
RVEF, %	51.7 ± 12.8	53.7 ± 12.5	48.0 ± 12.5	0.915	0.972 (0.954, 0.990)	0.002		
RV radial strain, %	39.0 ± 25.5	41.7 ± 27.3	34.1 ± 21.1	0.135	0.988 (0.977, 1.000)	0.045		
RV circumferential strain, %	−11.1 ± 8.5	−11.1 ± 5.8	−11.2 ± 12.1	0.533	1.001 (0.973, 1.031)	0.928		
RV longitudinal strain, %	−11.2 ± 6.4	−11.6 ± 4.5	−10.4 ± 9.0	0.277	1.045 (0.989, 1.103)	0.115		
Index RV mass, g/m^2	18.6 ± 7.6	18.3 ± 7.6	19.3 ± 7.5	0.913	1.015 (0.988, 1.044)	0.277		
RV LGE, negative/positive	44/151	36/89	8/62	0.005	2.753 (1.318. 5.752)	0.007		

Data are means ± SDs, medians with IQRs in parentheses, or numbers (%) of patients. Univariable Cox proportional hazard models were used, and a stepwise forward selection procedure (*P < 0.05 for entry)* was applied to create the final model listed here.

HR hazard ratio, *CI* confidence interval, *cTnI* cardiac troponin I, *NT-proBNP* N-terminal pro-B-type natriuretic peptide, *dFLC* serum immunoglobulin free light chain difference, *NYHA* New York Heart Association, *LA* left atrial, *LVEF* left ventricular ejection fraction, *LV* left ventricular, *ECV* extracellular volume fraction, *LGE* late gadolinium enhancement, *RA* right atrial, *RVEF* right ventricular ejection fraction, *RV* right ventricular, *SD* standard deviation, *IQR* interquartile range

Table 2
Multivariable Cox analysis with parametric mapping adjusted to univariate clinical and imaging predictors in all 195 patients.

	T2, > 44 ms		ECV, > 47%		Native T1, > 1468 ms	
	HR (95% CI)	*P*	HR (95% CI)	*P*	HR (95% CI)	*P*
Adjusted for Ln (NT-proBNP)	1.584 (0.928, 2.703)	0.092	1.146 (0.683, 1.924)	0.605	1.117 (0.667, 1.868)	0.675
Adjusted for cTnI	1.769 (1.034, 3.025)	0.037	1.811 (1.103, 2.972)	0.019	1.619 (0.982, 2.670)	0.059
Adjusted for hematologic response and cardiac response	1.998 (1.005, 3.972)	0.048	1.569 (0.839, 2.936)	0.158	1.456 (0.672, 2.781)	0.255
Adjusted for LV LGE	1.765 (1.036, 3.007)	0.037	1.426 (0.755, 2.692)	0.274	1.252 (0.714, 2.196)	0.433
Adjusted for LVEF	1.823 (1.071, 3.104)	0.027	1.640 (0.968, 2.781)	0.066	1.531 (0.926, 2.530)	0.097
Adjusted for LV longitudinal strain	1.818 (1.064, 3.107)	0.029	1.509 (0.875, 2.601)	0.139	1.454 (0.869, 2.433)	0.154

Multivariable Cox analysis included parametric mapping and other univariate predictors.
ECV extracellular volume fraction, *HR* hazard ratio, *CI* confidence interval, *cTnI* cardiac troponin I, *NT-proBNP* N-terminal pro-B-type natriuretic peptide, *LV* left ventricular, *LGE* late gadolinium enhancement, *LVEF* left ventricular ejection fraction

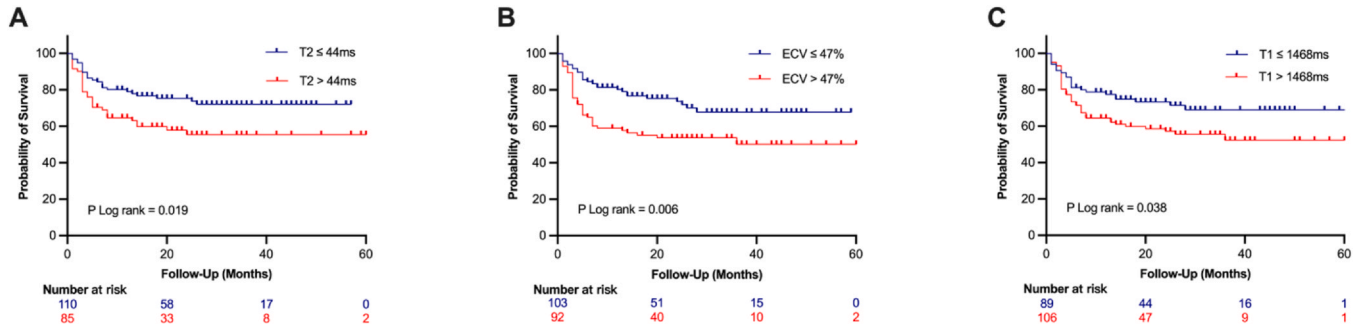

Fig. 2. Kaplan-Meier survival curves categorized by myocardial T2, ECV, and native T1 values in all AL amyloidosis patients. (A) Patients with T2 ≤44 ms and T2 > 44 ms differed significantly in survival probability (log rank, $P = 0.019$). (B) Patients with ECV ≤47% and ECV > 47% differed significantly in survival probability (log rank, $P = 0.006$). (C) Patients with T1 ≤1468 ms and T1 > 1468 ms differed significantly in survival probability (log rank, $P = 0.038$). *ECV* extracellular volume fraction

showed that T2 > 44 ms (HR 5.734, 95% CI 1.189–27.656, $P = 0.030$) was significantly associated with mortality in patients who achieved both deep hematologic response and cardiac response. Also, T2 > 44 ms remained independently prognostic after correcting for LV LGE and LV longitudinal strain (both, $P < 0.05$). Kaplan-Meier curve analysis demonstrated that patients with T2 > 44 ms had significantly lower rates for overall survival in AL amyloidosis patients achieving both deep hematologic response and cardiac response (both, log rank $P < 0.05$) than those with T2 ≤44 ms (Fig. 3, Supplemental Fig. 1); patients with T2 ≤44 ms reaped a median survival benefit of 3 months (27 months vs 24 months) and stage IV patients with T2 ≤44 ms reaped a median survival benefit of 21 months (44 months vs 23 months).

4. Discussion

In this study, we comprehensively evaluated the prognostic significance of CMR parametric mapping in AL amyloidosis patients. We found that CMR marker of myocardial edema (T2 value) bore independent predictive value for prognosis in AL amyloidosis patients. Moreover, T2 mapping provided additional prognostic information beyond LGE, LV function, and therapeutic response.

In this study, assessment of the extent of myocardial edema by T2 mapping showed potential to improve the therapeutic strategies for patients with AL amyloidosis. As previously reported, the recently proposed criteria of hematologic and cardiac responses provided a sharp discrimination of outcome in international populations of patients [19,20]. We found that T2 provided prognostic association with mortality over hematologic response and cardiac response in the overall cohort and in the Mayo stage IV subgroup. T2 > 44 ms was independently prognostic for mortality after correcting for cardiac response among patients who reached a deep hematologic response (at least VGPR). Importantly, when we looked at those patients who reached both deep hematologic response and cardiac response, a myocardial T2 cutoff value of 44 ms allowed to identify those patients with significantly increased risk for mortality in this subgroup. Cardiotoxicity-related edema superimposed on amyloid infiltration might lead to worsened prognosis despite successful chemotherapy. Our findings highlight the role of T2 mapping in individuals who had already achieved a deep therapeutic response, suggesting that consideration should be given to assessment of myocardial edema in these patients. In this scenario, CMR could substantially improve patient selection for adjunctive therapies to promote the repair of myocardial edema and for the intensification of medical therapy.

Our data underscore that assessment of myocardial edema is of particular prognostic importance. In vitro and in vivo studies demonstrated that amyloid proteins have potent cardiotoxicity to induce mitochondrial dysfunction of the myocardium together with deposition effects [21,22], suggesting myocardial edema as a biomarker. We observed that T2 value was a potent CMR predictor of hard clinical events, portending to progressively increased risk of mortality. One previous study indicated myocardial T2 as a predictor of prognosis in AL amyloidosis [8], while another study showed that myocardial T2 could differentiate AL amyloidosis from transthyretin amyloidosis but did not impact survival [23]. Our findings are in accordance with the former and further assessed the prognostic value through subgroup analysis. Thus, sole serum FLC clearance might not promise prolonged survival, additional efforts should be focused on myocardial cell protection against light chain or AL amyloidosis fibril toxicity or differing rates of amyloid deposition.

We found that T2 > 44 ms, ECV > 47%, and native T1 > 1468 ms were all significantly prognostic in AL amyloidosis, but they were no longer statistically significant after adjustment for NT-proBNP. NT-proBNP test is widely available and works as an important prognostic marker in the patient care, while CMR parametric mapping provided limited prognostic information over NT-proBNP. From the perspective of efficiency and productivity, we still need to find the right subpopulations to get CMR scans for the right reasons. Clinicians need to determine the necessity of CMR on an individual patient basis. The

Table 3
Univariable and multivariable Cox analysis with parametric mapping in patients with different Mayo stages.

	T2, > 44 ms		ECV, > 47%		Native T1, > 1468 ms	
	HR (95% CI)	*P*	HR (95% CI)	*P*	HR (95% CI)	*P*
Mayo I						
Univariable	0.034 (0.001, 28.142)	0.643	0.042 (0.001, 27.500)	0.747	0.031 (0.001, 53.864)	0.612
Adjusted for Ln (NT-proBNP)	0.004 (0.002, 27.688)	0.958	0.007 (0.002, 25.715)	0.993	0.005 (0.001, 32.598)	0.984
Adjusted for cTnI	0.002 (0.001, 19.109)	0.986	0.002 (0.001, 29.023)	0.993	0.003 (0.002, 27.728)	0.984
Adjusted for hematologic response and cardiac response	0.440 (0.001, 38.173)	0.997	0.990 (0.001, 66.871)	0.999	0.990 (0.001, 67.378)	0.999
Adjusted for LV LGE	0.010 (0.001, 17.259)	0.985	0.008 (0.001, 42.517)	0.992	0.005 (0.001, 11.326)	0.480
Adjusted for LVEF	0.002 (0.001, 11.105)	0.985	0.003 (0.001, 21.866)	0.993	0.009 (0.001, 12.875)	0.984
Adjusted for LV longitudinal strain	0.010 (0.001, 14.358)	0.985	0.005 (0.001, 14.825)	0.993	0.006 (0.001, 14.298)	0.984
Mayo II						
Univariable	2.429 (0.791, 7.466)	0.121	2.825 (0.972, 8.213)	0.057	1.465 (0.513, 4.182)	0.475
Adjusted for Ln (NT-proBNP)	2.029 (0.634, 6.496)	0.233	1.584 (0.410, 6.121)	0.504	1.024 (0.323, 3.243)	0.968
Adjusted for cTnI	2.438 (0.791, 7.514)	0.121	4.270 (0.001, 14.979)	0.809	3.623 (0.001, 24.842)	0.821
Adjusted for hematologic response and cardiac response	2.124 (0.490, 9.214)	0.314	9.848 (1.453, 66.745)	0.019	2.847 (0.567, 14.292)	0.204
Adjusted for LV LGE	2.457 (0.798, 7.567)	0.117	3.107 (0.740, 13.052)	0.122	1.028 (0.293, 3.605)	0.965
Adjusted for LVEF	2.397 (0.778, 7.382)	0.128	5.318 (1.093, 25.864)	0.038	1.350 (0.458, 3.978)	0.586
Adjusted for LV longitudinal strain	2.665 (0.861, 8.251)	0.089	2.877 (0.634, 13.056)	0.171	1.225 (0.409, 3.667)	0.717
Mayo III						
Univariable	1.885 (0.730, 4.867)	0.190	1.581 (0.697, 3.584)	0.273	1.161 (0.505, 2.671)	0.725
Adjusted for Ln (NT-proBNP)	2.054 (0.793, 5.320)	0.138	1.307 (0.571, 2.992)	0.526	0.936 (0.402, 2.177)	0.877
Adjusted for cTnI	1.618 (0.596, 4.390)	0.345	1.531 (0.671, 3.491)	0.312	1.085 (0.466, 2.52*)	0.849
Adjusted for hematologic response and cardiac response	1.952 (0.514, 7.403)	0.326	0.922 (0.305, 2.786)	0.885	1.664 (0.445, 6.227)	0.449
Adjusted for LV LGE	1.893 (0.733, 4.890)	0.188	1.818 (0.602, 5.490)	0.289	1.148 (0.480, 2.747)	0.756
Adjusted for LVEF	1.811 (0.702, 4.674)	0.220	1.596 (0.690, 3.693)	0.275	1.146 (0.493, 2.662)	0.751
Adjusted for LV longitudinal strain	1.827 (0.707, 4.725)	0.214	1.611 (0.680, 3.815)	0.278	1.143 (0.488, 2.675)	0.758
Mayo IV						
Univariable	1.380 (0.596, 3.196)	0.452	0.799 (0.347, 1.841)	0.599	1.566 (0.654, 3.750)	0.314
Adjusted for Ln (NT-proBNP)	1.300 (0.559, 3.022)	0.542	0.853 (0.369, 1.970)	0.709	1.527 (0.635, 3.669)	0.344
Adjusted for cTnI	1.327 (0.567, 3.103)	0.515	0.737 (0.316, 1.716)	0.479	1.584 (0.660, 3.803)	0.303
Adjusted for hematologic response and cardiac response	4.177 (1.122, 15.545)	0.033	0.520 (0.169, 1.598)	0.253	0.594 (0.175, 2.018)	0.404
Adjusted for LV LGE	1.391 (0.593, 3.262)	0.448	0.729 (0.265, 2.080)	0.555	1.976 (0.676, 5.777)	0.213
Adjusted for LVEF	1.528 (0.647, 3.612)	0.334	0.738 (0.319, 1.705)	0.477	1.532 (0.639, 3.676)	0.339
Adjusted for LV longitudinal strain	1.647 (0.662, 4.096)	0.283	0.882 (0.366, 2.123)	0.882	1.855 (0.729, 4.722)	0.195

Multivariable Cox analysis included parametric mapping and other univariate predictors.
ECV extracellular volume fraction, *HR* hazard ratio, *CI* confidence interval, *cTnI* cardiac troponin I, *NT-proBNP* N-terminal pro-B-type natriuretic peptide, *LV* left ventricular, *LGE* late gadolinium enhancement, *LVEF* left ventricular ejection fraction

Table 4
Univariable and multivariable Cox analysis with parametric mapping in patients achieving hematologic and cardiac response.

	T2, > 44 ms		ECV, > 47%		Native T1, > 1468 ms	
	HR (95% CI)	*P*	HR (95% CI)	*P*	HR (95% CI)	*P*
Deep hematologic response						
Univariable	2.723 (0.890, 8.331)	0.079	1.842 (0.639, 5.310)	0.258	2.397 (0.752, 7.6450	0.140
Adjusted for Ln (NT-proBNP)	1.724 (0.551, 5.395)	0.349	0.618 (0.197, 1.938)	0.618	0.973 (0.269, 3.527)	0.967
Adjusted for cTnI	2.708 (0.882, 8.314)	0.082	1.523 (0.657, 3.529)	0.326	1.971 (0.8815, 4.767)	0.132
Adjusted for cardiac response	6.611 (1.723, 25.361)	0.006	1.873 (0.644, 5.445)	0.249	2.956 (0.917, 9.531)	0.070
Adjusted for LV LGE	2.538 (0.826, 7.796)	0.104	1.410 (0.365, 5.447)	0.618	2.024 (0.543, 7.537)	0.293
Adjusted for LVEF	2.319 (0.758, 7.100)	0.141	1.030 (0.327, 3.250)	0.959	1.747 (0.537, 5.686)	0.354
Adjusted for LV longitudinal strain	2.381 (0.771, 7.354)	0.132	1.080 (0.328, 3.551)	0.899	1.720 (0.517, 5.725)	0.376
Deep hematologic response and cardiac response						
Univariable	5.734 (1.189, 27.656)	0.030	1.450 (0.419, 5.011)	0.557	2.289 (0.592, 8.855)	0.230
Adjusted for Ln (NT-proBNP)	3.227 (0.657, 15.836)	0.149	0.421 (0.114, 1.552)	0.194	0.720 (0.153, 3.391)	0.678
Adjusted for cTnI	0.977 (0.085, 11.235)	0.985	0.433 (0.028, 6.740)	0.550	14.892 (0.001, 32.228)	0.929
Adjusted for LV LGE	5.292 (1.095, 25.582)	0.038	0.837 (0.197, 3.550)	0.810	1.684 (0.375, 7.556)	0.496
Adjusted for LVEF	4.705 (0.972, 22.763)	0.054	0.869 (0.230, 3.290)	0.836	1.794 (0.457, 7.047)	0.402
Adjusted for LV longitudinal strain	5.095 (1.049, 24.747)	0.043	0.945 (0.232, 3.850)	0.937	1.815 (0.443, 7.436)	0.408

Multivariable Cox analysis included parametric mapping and other univariate predictors.
ECV extracellular volume fraction, *HR* hazard ratio, *CI* confidence interval, *cTnI* cardiac troponin I, *NT-proBNP* N-terminal pro-B-type natriuretic peptide, *LV* left ventricular, *LGE* late gadolinium enhancement, *LVEF* left ventricular ejection fraction

current study identified the prognostic value of T2 mapping in patients with a deep therapeutic response. Large cooperative studies are necessary to further validate the impact of multiparametric CMR in subpopulations of AL amyloidosis.

5. Limitations

Several limitations of this research should be acknowledged. First, this is a single-center study. Limited events constrained the number of

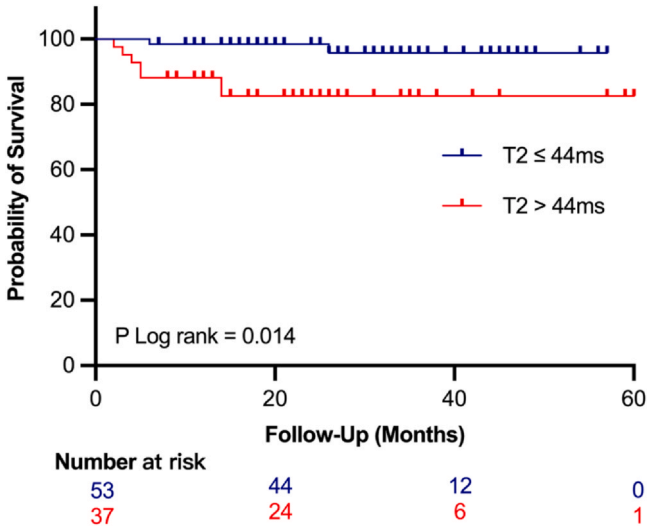

Fig. 3. Kaplan-Meier survival curve categorized by myocardial T2 value in AL amyloidosis patients achieving both deep hematologic response and cardiac response. Patients with T2 ≤ 44 ms and T2 > 44 ms differed significantly in survival probability (log rank, $P = 0.014$), with a median survival benefit of 3 months (27 months vs 24 months)

factors to be included in the multivariate models. Second, there was no histological evidence to verify our findings, though other studies have provided similar results. Third, recruitment was terminated in 2019 before newer therapies such as daratumumab emerged. Fourth, the cutoffs obtained from the 195 patients may not represent the ground truth, which should ideally be derived from large populations. Large cooperative studies are necessary to further validate the impact of multiparametric CMR in AL amyloidosis.

6. Conclusions

In conclusion, the extent of myocardial edema by T2 mapping is an independent prognostic predictor in AL amyloidosis. Myocardial edema assessment identified patients in need of adjunctive therapies for myocardial cell protection, which is of particular prognostic significance in patients with deep therapeutic response.

Funding

This study was supported by the National Natural Science Foundation of China (grants 82325026, 82020108018, 82202134) and National High Level Hospital Clinical Research Funding (grants 2022-PUMCH-B-027, 2022-PUMCH-D-002).

Author contributions

All authors significantly contributed to this work, read and approved the final manuscript.

Ethics approval and consent

The institutional ethics committee at Peking Union Medical College Hospital (Beijing, China) approved the study. All participants were required to provide written informed consent before recruitment.

Consent for publication

Written informed consent was obtained from all participants for inclusion of their data in publications.

Availability of data and materials

The datasets used or analyzed during the current study are available from the corresponding author upon reasonable request.

Declaration of competing interests

The authors declare that they have no known competing financial interests or personal relationships that could have appeared to influence the work reported in this paper.

Acknowledgements

The authors thank each of the study subjects for their participation.

Appendix A. Supporting information

Supplementary data associated with this article can be found in the online version at doi:10.1016/j.jocmr.2024.101135.

References

[1] Falk RH, Comenzo RL, Skinner M. The systemic amyloidoses. N Engl J Med 1997;337:898–909.
[2] Maurer MS, Elliott P, Comenzo R, Semigran M, Rapezzi C. Addressing common questions encountered in the diagnosis and management of cardiac amyloidosis. Circulation 2017;135:1357–77.
[3] Palladini G, Dispenzieri A, Gertz MA, Kumar S, Wechalekar A, Hawkins PN, et al. New criteria for response to treatment in immunoglobulin light chain amyloidosis based on free light chain measurement and cardiac biomarkers: impact on survival outcomes. J Clin Oncol 2012;30:4541–9.
[4] Comenzo RL, Reece D, Palladini G, Seldin D, Sanchorawala V, Landau H, et al. Consensus guidelines for the conduct and reporting of clinical trials in systemic light-chain amyloidosis. Leukemia 2012;26:2317–25.
[5] Kumar S, Dispenzieri A, Lacy MQ, Hayman SR, Buadi FK, Colby C, et al. Revised prognostic staging system for light chain amyloidosis incorporating cardiac biomarkers and serum free light chain measurements. J Clin Oncol 2012;30:989–95.
[6] Messroghli DR, Moon JC, Ferreira VM, Grosse-Wortmann L, He T, Kellman P, et al. Clinical recommendations for cardiovascular magnetic resonance mapping of T1, T2, T2* and extracellular volume: a consensus statement by the Society for Cardiovascular Magnetic Resonance (SCMR) endorsed by the European Association for Cardiovascular Imaging (EACVI). J Cardiovasc Magn Reson 2017;19:75.
[7] Baggiano A, Boldrini M, Martinez-Naharro A, Kotecha T, Petrie A, Rezk T, et al. Noncontrast magnetic resonance for the diagnosis of cardiac amyloidosis. JACC Cardiovasc Imaging 2020;13:69–80.
[8] Kotecha T, Martinez-Naharro A, Treibel TA, Francis R, Nordin S, Abdel-Gadir A, et al. Myocardial edema and prognosis in amyloidosis. J Am Coll Cardiol 2018;71:2919–31.
[9] Knight DS, Zumbo G, Barcella W, Steeden JA, Muthurangu V, Martinez-Naharro A, et al. Cardiac structural and functional consequences of amyloid deposition by cardiac magnetic resonance and echocardiography and their prognostic roles. JACC Cardiovasc Imaging 2019;12:823–33.
[10] Raina S, Lensing SY, Nairooz RS, Pothineni NV, Hakeem A, Bhatti S, et al. Prognostic value of late gadolinium enhancement CMR in systemic amyloidosis. J Am Coll Cardiol Imaging 2016;9:1267–77.
[11] Fontana M, Pica S, Reant P, Abdel-Gadir A, Treibel TA, Banypersad SM, et al. Prognostic value of late gadolinium enhancement cardiovascular magnetic resonance in cardiac amyloidosis. Circulation 2015;132:1570–9.
[12] Banypersad SM, Fontana M, Maestrini V, Sado DM, Captur G, Petrie A, et al. T1 mapping and survival in systemic light-chain amyloidosis. Eur Heart J 2015;36:244–51.
[13] Dispenzieri A, Gertz MA, Kyle RA, Lacy MQ, Burritt MF, Therneau TM, et al. Serum cardiac troponins and N-terminal pro-brain natriuretic peptide: a staging system for primary systemic amyloidosis. J Clin Oncol 2004;22:3751–7.
[14] Merlini G, Lousada I, Ando Y, Dispenzieri A, Gertz MA, Grogan M, et al. Rationale, application and clinical qualification for NT-proBNP as a surrogate end point in pivotal clinical trials in patients with AL amyloidosis. Leukemia 2016;30:1979–86.
[15] Kramer CM, Barkhausen J, Flamm SD, Kim RJ, Nagel E. Society for Cardiovascular Magnetic Resonance Board of Trustees Task Force on Standardized P. Standardized cardiovascular magnetic resonance (CMR) protocols 2013 update. J Cardiovasc Magn Reson 2013;15:91.
[16] Schulz-Menger J, Bluemke DA, Bremerich J, Flamm SD, Fogel MA, Friedrich MG, et al. Standardized image interpretation and post processing in cardiovascular magnetic resonance: Society for Cardiovascular Magnetic Resonance (SCMR) board of trustees task force on standardized post processing. J Cardiovasc Magn Reson 2013;15:35.
[17] Li X, Huang S, Han P, Zhou Z, Azab L, Lu M, et al. Nonenhanced chemical exchange saturation transfer cardiac magnetic resonance imaging in patients with amyloid light-chain amyloidosis. J Magn Reson Imaging 2022;55:567–76.

[18] Lin L, Li X, Feng J, Shen KN, Tian Z, Sun J, et al. The prognostic value of T1 mapping and late gadolinium enhancement cardiovascular magnetic resonance imaging in patients with light chain amyloidosis. J Cardiovasc Magn Reson 2018;20:2.
[19] Manwani R, Foard D, Mahmood S, Sachchithanantham S, Lane T, Quarta C, et al. Rapid hematologic responses improve outcomes in patients with very advanced (stage IIIb) cardiac immunoglobulin light chain amyloidosis. Haematologica 2018;103:e165–8.
[20] Basset M, Milani P, Foli A, Nuvolone M, Benvenuti P, Nanci M, et al. Early cardiac response is possible in stage IIIb cardiac AL amyloidosis and is associated with prolonged survival. Blood 2022;140:1964–71.
[21] Guan J, Mishra S, Qiu Y, Shi J, Trudeau K, Las G, et al. Lysosomal dysfunction and impaired autophagy underlie the pathogenesis of amyloidogenic light chain-mediated cardiotoxicity. EMBO Mol Med 2015;7:688.
[22] Brenner DA, Jain M, Pimentel DR, Wang B, Connors LH, Skinner M, et al. Human amyloidogenic light chains directly impair cardiomyocyte function through an increase in cellular oxidant stress. Circ Res 2004;94:1008–10.
[23] Ridouani F, Damy T, Tacher V, Derbel H, Legou F, Sifaoui I, et al. Myocardial native T2 measurement to differentiate light-chain and transthyretin cardiac amyloidosis and assess prognosis. J Cardiovasc Magn Reson 2018;20:58.